

Article

Influence of Chemical Surface Characteristics of Ammonium-Modified Chilean Zeolite on Oak Catalytic Pyrolysis

Serguei Alejandro-Martín ^{1,2,*} , Adán Montecinos Acaricia ², Cristian Cerda-Barrera ³ and Hatier Díaz Pérez ³

¹ Departamento de Ingeniería en Maderas, Facultad de Ingeniería, Universidad del Bío-Bío (UBB), Concepción 4030000, Chile

² Nanomaterials and Catalysts for Sustainable Processes (NanoCatpPS), Universidad del Bío-Bío (UBB), Concepción 4030000, Chile; amontecinos@ubiobio.cl

³ Departamento de Procesos Industriales, Facultad de Ingeniería, Universidad Católica de Temuco, Temuco 4780000, Chile; ccerda@uct.cl (C.C.-B.); hatierdiazp@gmail.com (H.D.P.)

* Correspondence: salejandro@ubiobio.cl; Tel.: +56-41-311-1168

Received: 10 March 2019; Accepted: 27 April 2019; Published: 21 May 2019



Abstract: The influence of chemical surface characteristics of Chilean natural and modified zeolites on Chilean Oak catalytic pyrolysis was investigated in this study. Chilean zeolite samples were characterised by nitrogen absorption at 77 K, X-ray powder diffraction (XRD), and X-ray fluorescence (XRF). The nature and strength of zeolite acid sites were studied by diffuse reflectance infrared Fourier transform (DRIFT), using pyridine as a probe molecule. Experimental pyrolysis was conducted in a quartz cylindrical reactor and bio-oils were obtained by condensation of vapours in a closed container. Chemical species in bio-oil samples were identified by a gas chromatography/mass spectrophotometry (GC/MS) analytical procedure. Results indicate that after the ionic exchange treatment, an increase of the Brønsted acid site density and strength was observed in ammonium-modified zeolites. Brønsted acids sites were associated with an increment of the composition of ketones, aldehydes, and hydrocarbons and to a decrease in the composition of the following families (esters; ethers; and acids) in obtained bio-oil samples. The Brønsted acid sites on ammonium-modified zeolite samples are responsible for the upgraded bio-oil and value-added chemicals, obtained in this research. Bio-oil chemical composition was modified when the pyrolysis-derived compounds were upgraded over a 2NHZ zeolite sample, leading to a lower quantity of oxygenated compounds and a higher composition of value-added chemicals.

Keywords: chilean natural zeolite; Brønsted acid sites; bio-oil upgrade; catalytic pyrolysis

1. Introduction

Nowadays, energy is a crucial issue in the global economy; energy drives industrialisation and agricultural activities. As the pillar of growth and development, energy is mainly obtained from fossil fuel, the primary energy source used worldwide. However, there are some issues which are actively debated nowadays: world sustainability; global warming; democratisation of the energy sources; access to cheap and reliable energy; and the physical or economic scarcity of petroleum as the prime energy source [1]. Traditionally, the incremental energy demand has been satisfied using fossil fuels, but in the coming years that energy will be substituted by low carbon and ultimately zero-carbon [2]. Usage of fossil fuel energy release more than 30 billion tons of CO₂ each year, exceeding the level that can be recycled by nature, contributing to global warming [3]. Thus, several countries are launching strategies to develop new alternative energies (Aeolic, solar, hydroelectric, biomass) to decrease current

polluting matrices, through scientific and technological development and human resources training programs [4].

Among the alternative energies, biomass contributes to about 12% of the world primary energy supply, and it is recognised as the leading renewable substitute of fossil oil [5]. Biomass could be used as a sustainable source of bioenergy; bio-based products and add-value biochemicals, through thermochemical, biological, chemical conversion, and physical processes [6]. Currently, the thermochemical conversion of biomass is one of the most promising processes to obtain sustainable fuels to solve environmental problems caused by the over-consumption of fossil fuels [7]. Derived products (biochar, bio-oil, and fuel gas) from biomass pyrolysis offers an alternative way to obtain renewable fuel resources [5]. Nevertheless, upgrading processes are necessary as a consequence of bio-oil low heating value, high viscosity, water content, instability, and corrosiveness [8]. Among those processes, zeolite cracking becomes a remarkable way to reduce the oxygen content of bio-oil samples, through decarbonylation, decarboxylation, dehydration, oligomerization, isomerization, and dehydrogenation reactions [9]. Catalytic cracking of biomass pyrolysis vapours and bio-oil promotes oxygen removal as CO, CO₂, and H₂O, increasing the possibilities of bio-oil usage as a fuel source [10]. Synthetic zeolites (A, Y, H-Y, ZSM-5, and H-ZSM-5) are preferred catalyst in upgrading processes these days. They are claimed as responsible for the increase of desirable chemical compounds (phenols, furans, aromatics, and hydrocarbons) after bio-oil upgrading processes [11,12]. However, synthetic zeolites high cost (e.g., ZSM-5 -> \$120/Kg, Y -> \$180/Kg, MCM-41 -> \$1190/Kg, β-zeolite -> \$1065/Kg) constitutes a non-minor disadvantage [13].

In contrast, natural zeolites are cheap and plentiful, showing prices in the range of \$20 to \$100 per metric ton (in the US). Worldwide, natural clinoptilolite showed an average value of \$242 per metric ton and even 40% lower for natural zeolites from China [1]. In addition, United States resources of natural zeolites have been estimated by 120 million tons of clinoptilolite, chabazite, erionite, mordenite, and phillipsite in near-surface deposits [14]. Although some zeolites are found in nature, they have limited application in catalytic pyrolysis due to their lower performance compared to synthetic ones. Nevertheless, the activity of natural zeolites can be significantly improved through appropriate modifications [15]. Thus, researchers have conducted some investigations incorporating natural zeolites as the catalyst in biomass catalytic pyrolysis studies [16–18]. An increase of bio-oil yield was linked to the usage of natural zeolite (clinoptilolite) as a catalyst in *Euphorbia rigida* pyrolysis [19]. Ammonium chloride modified zeolite (clinoptilolite) was used previously in peanut shells pyrolysis. Ionic exchange procedure enhances Brønsted acid sites (bridging hydroxyls connected to framework aluminium atoms) on the zeolites' internal structure, leading to deoxygenation of the obtained bio-oil samples [9]. Metal oxides nanoparticles (NiO, ZnO, Cu₂O, CaO, and MgO) were incorporated into natural clinoptilolite elsewhere, to study catalytic activity of zeolites samples in the pyrolysis of hardwood lignin. Incorporated nanoparticles on a zeolite framework act as Brønsted and Lewis acid sites, leading to an increase of phenol yield in bio-oil samples [20,21].

The studies above have been conducted to enhance natural zeolites catalytic activity looking to increase bio-oil yield, identify bio-oil derivatives that contribute to bio-oil stability or to obtain bio-based raw materials for chemical industries [22,23]. Nevertheless, the catalytic activity of Chilean natural and modified zeolite on Chilean Oak pyrolysis and their influence on the chemical composition has not been sufficiently investigated yet. Consequently, this research is focused on the analysis of the influence of chemical surface characteristics of Chilean natural zeolite on the composition of bio-oil obtained from the pyrolysis of Chilean Native Oak.

2. Results and Discussion

2.1. Biomass and Natural Zeolite Characterization

Lignocellulosic biomass is a complex composite material where the main constituents are cellulose, hemicellulose, lignin, water, extractives, and inorganic (ash) compounds. Linkage of components

above provides structural strength and flexibility to lignocellulosic species [24]. As the percentage of main components varies from one species to other, Chilean oak was characterised according to detailed procedures (see Materials and Methods). The results of proximate (dry basis), ultimate, and elemental analyses are summarised in Table 1.

Table 1. Chilean Oak proximate (dry basis), ultimate, and elemental analyses.

VM [wt%]	FC [wt%]	Ash [wt%]	GCV ^a [MJ·kg ⁻¹]	GCV ^b [MJ·kg ⁻¹]	Cellulose [%]	Hemicellulose [%] ^c	Lignin [%]	Extractives [%]	C	H	O	N
85.74	12.62	1.64	20.72	24.93	35.38	35.55	27.10	1.97	47.30	6.36	46.34	-

Volatile Matter (VM), Fixed Carbon (FC) Gross calorific value (GCV). ^a Dried at 378 K, 12 h. ^b Bio-char from pyrolysis at 623 K, 30 min. ^c by difference.

Taking into consideration that the main structural chemical components (carbohydrate polymers and oligomers) constitute about 65 to 75%, lignin 18 to 35%, and organic extractives and inorganic minerals usually 4 to 10%, the summarised results of Table 1 are in accordance with reported articles elsewhere [25].

Thermogravimetric analysis of biomass was conducted, in a nitrogen atmosphere, to study the thermal behavior of Chilean Oak. TG/DTG/DTA (thermogravimetric/derivative thermogravimetric/differential thermogravimetric analysis) profiles show an active pyrolysis (hemicellulose and cellulose degradation) zone around 476 to 668 K, and passive pyrolysis (lignin degradation) zone at $T > 668$ K. Maximum degradation of hemicellulose occurs at 576 K and cellulose maximum degradation rate ($0.01 \text{ mg}\cdot\text{s}^{-1}$) was achieved at 628 K, removing 59% of the initial mass at this temperature. Thermogravimetric profiles of Chilean Oak were reported in a previous article [18]. Considering the above, pyrolysis experiments were conducted at 723 K to assure the complete thermal transformation of the biomass.

Natural zeolite was characterized by nitrogen absorption at 77 K, X-ray powder diffraction (XRD) and X-ray fluorescence (XRF), as mentioned in the Materials and Methods section. Table 2 summarises physical–chemical characterization results of natural and modified zeolite samples.

Table 2. Physico-chemical characterization of natural and modified Chilean zeolite samples.

Sample	S ^a [m ² ·g ⁻¹]	SiO ₂ ^b [% w/w]	Al ₂ O ₃ ^b [% w/w]	Na ₂ O ^b [% w/w]	CaO ^b [% w/w]	K ₂ O ^b [% w/w]	MgO ^b [% w/w]	TiO ₂ ^b [% w/w]	Fe ₂ O ₃ ^b [% w/w]	MnO ^b [% w/w]	P ₂ O ₅ ^b [% w/w]	CuO ^b [% w/w]	Si/Al
NZ	168.17	71.61	15.18	2.0	3.43	2.03	0.74	0.61	3.99	0.06	0.12	0.03	4.72
NHZ	228.21	74.39	15.42	0.83	2.16	1.99	0.61	0.57	3.57	0.04	0.08	-	4.82
2NHZ	219.14	75.27	15.59	0.46	1.67	1.92	0.59	0.60	3.53	0.05	0.08	-	4.83

^a Surface area in [m²·g⁻¹]; ^b by XRF (X-ray fluorescence) [% w/w].

Surface areas were obtained by fitting the Langmuir adsorption model to nitrogen adsorption registered data. Zeolite samples were outgassed at 623 K for 12 h before all adsorption measurements. Nitrogen adsorption isotherms exposed a combination of type I and IV characteristic isotherms, according to the International Union of Pure and Applied Chemistry (IUPAC) classification [26]. A rapid filling of micropores was registered at low relative pressure (P/P_0) values and an increase of adsorbed nitrogen at ($P/P_0 \approx 0.9$), possibly due to mesopores. Registered data are in agreement with other results reported elsewhere [27,28].

As Table 2 shows, an increase of surface area was registered for ammonium-exchanged samples, and it could be associated with the decrease of compensation cations (Ca, Na, K, and Mg) composition in the zeolite framework. Lower compensation cations compositions improved nitrogen diffusion on the zeolite pore structure [29]. XRD patterns of natural and ammonium-modified zeolite samples indicated a high degree of crystallinity. Characteristic peaks of clinoptilolite, mordenite, and quartz structures were observed in X-ray patterns, as reported previously [29]. Comparison of registered patterns corroborates that applied ion-exchange procedure did not bring any significant changes in the zeolite framework, as XRD patterns are almost identical. Mordenite main channels (perpendicular 12 MR pores, 6.7×7.0 Å; parallel 8 MR pores, 2.9×5.7 Å; and side pockets, 2.9 Å diameter) are responsible

for diffusivity and accessibility of target compounds to surface acid sites. Characterization results were similar to other Chilean natural zeolites reported previously [30].

2.2. Characterization of Acid Sites by Pyridine-DRIFT

Figure 1 shows collected diffuse reflectance infrared Fourier transform (DRIFT) spectra of pyridine-saturated natural and modified zeolites after a thermal desorption procedure to evaluate Brønsted and Lewis acid site strength. Pyridine-saturated samples were outgassed (at vacuum) before infra-red experiments, increasing the temperature to 573 K from room temperature (RT). Each spectrum was recorded at 293 K after the cooling of zeolite samples. DRIFT technique allowed the identification of Brønsted (Py-B) and Lewis (Py-L) acid sites in zeolite samples, following the interaction of the pyridine molecule with Brønsted acid sites (near 1540 cm^{-1}) and Lewis acid sites (near 1450 cm^{-1}) [31–34]. The registered bands at 1456 cm^{-1} were associated with adsorbed pyridine at the Lewis acid sites. Likewise, registered bands at 1539 cm^{-1} were linked to Brønsted acid sites, whereas the band at 1488 cm^{-1} could be attributed to both acid sites [35,36].

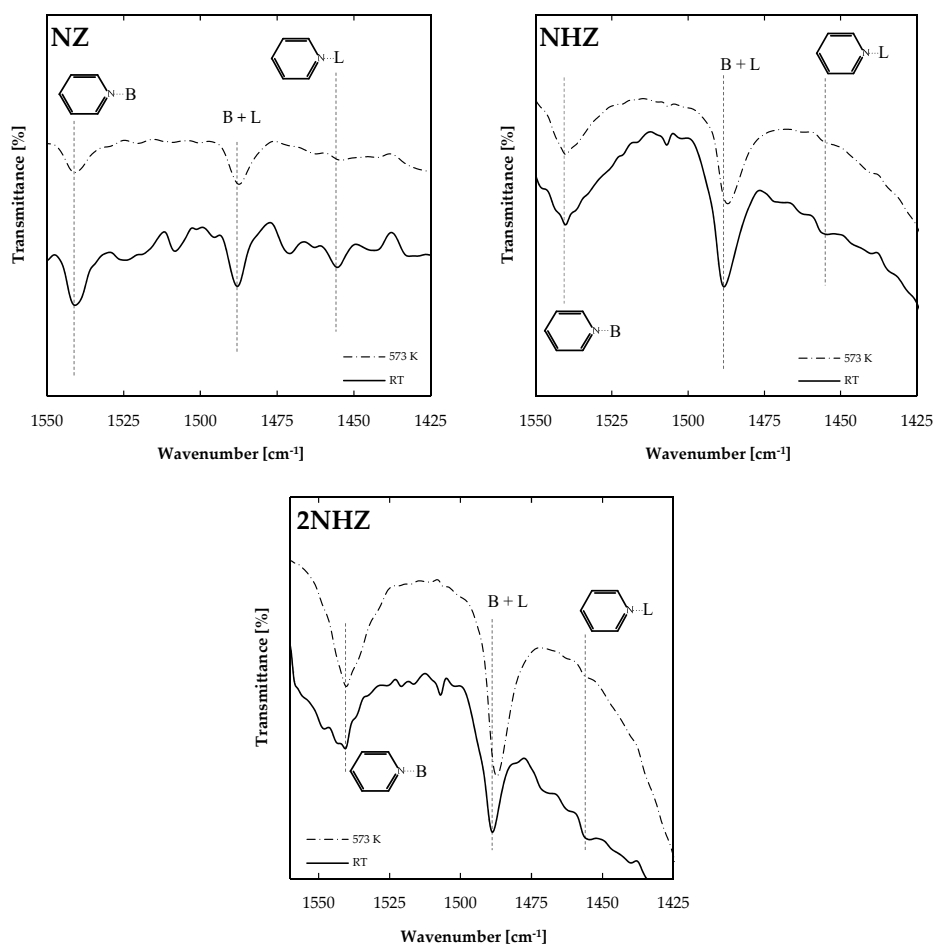


Figure 1. Diffuse reflectance infrared Fourier transform (DRIFT) spectrum of adsorbed pyridine on natural and modified zeolite.

To quantify acid sites, the ratio of Brønsted (B) and Lewis (L) acid sites (AS) was calculated using the following Equation (1):

$$\frac{C_{BAS}}{C_{LAS}} = \left(\frac{1.73}{1.23}\right) \left(\frac{I_{BAS}}{I_{LAS}}\right) \quad (1)$$

where I_{BAS} and I_{LAS} represent the intensity of absorption bands at 1540 and 1456 cm^{-1} , and 1.73 and 1.23 are the extinction coefficients, as reported previously [37,38]. The obtained C_{BAS}/C_{LAS} ratios are summarised in Table 3.

Table 3. Acid sites ratio of natural and modified zeolite samples.

Temperature [K]	C_{BAS}/C_{LAS} Ratio		
	NZ	NHZ	2NHZ
293	0.97	1.71	2.74
573	1.34	1.36	1.42

The registered data in Table 3 indicates that higher BAS/LAS ratio was observed in ammonium-modified zeolite samples, corroborating that ionic exchange incorporates new Brønsted acid sites at the zeolite framework. Moreover, as the heating temperature increases from 298 K to 573 K, weak acid sites disappear, and only strong acid sites still retain the pyridine probe molecule. Thus, registered peaks after the 573 K outgassing procedure, reveal a higher density of stronger Brønsted acid sites on the 2NHZ sample, in comparison to the NZ sample. As demonstrated here, the modification process can modify the acidity of natural zeolites to increase Brønsted acid sites' density.

2.3. Influence of Chemical Surface Characteristics of Zeolite Samples in Bio-Oil Composition

A semi-quantitative gas chromatography/mass spectrophotometry (GC/MS) analysis of fractionated bio-oil samples was conducted (See Materials and Methods) to identify primary chemical compounds of representative families, to evaluate the influence of chemical surface characteristics of natural and modified zeolite samples on the chemical composition of obtained bio-oil samples. Results are represented in Figure 2.

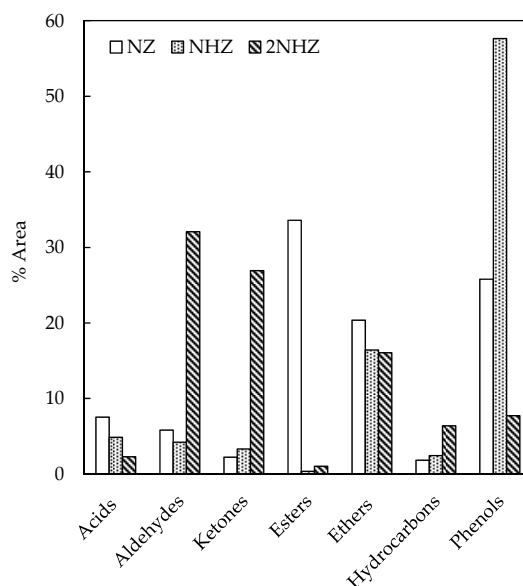
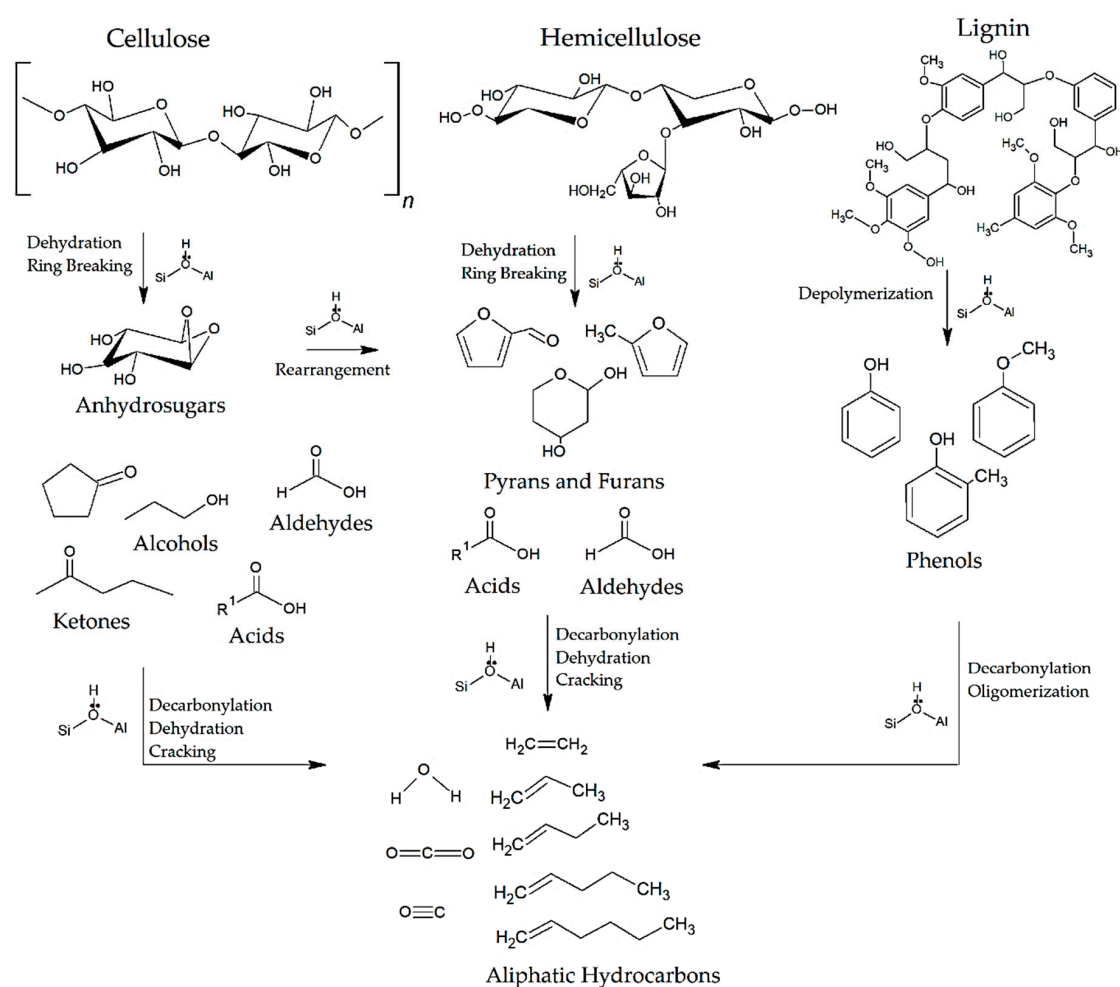


Figure 2. Primary chemical composition of bio-oil samples. Experiment Conditions: Pyrolysis Temp: 723 K; Cat./Oak ratio: 4; Flow 120 $\text{ml}\cdot\text{min}^{-1}$; Ramp rate 10 $\text{K}\cdot\text{min}^{-1}$.

Figure 2 shows a decrease in the composition of the following families (esters, ethers, and acids) as a result of the catalytic activity of modified (NHZ and 2NHZ) zeolite samples. Esters, ethers, and other oxygenated compounds are unwanted species, as they decrease the bio-oil heating value. Furthermore, a lower acid composition is highly desirable in bio-oil samples, taking into consideration that lower pH promotes aging reactions during the storage of samples.

Compositional fluctuations in stored bio-oil samples are due to potential aging reactions (e.g., alcohols reacting with organic acids forming esters and water, aldehydes reacting with each other to form polyacetal oligomers and polymers, aldehydes or ketones reacting with water to form hydrates, alcohols reacting with aldehydes forming hemiacetals, aldehydes and alcohols reacting to form acetals, and phenol/aldehyde reactions), as suggested by other studies [18,39]. Therefore, a lower content of acids, esters, ethers, and phenols will contribute to higher bio-oil stability during storage. Bio-Oil stability becomes a crucial matter when considering it as a potential substitute for fossil fuel.

On the other hand, an increase in the composition of aldehydes, ketones, and hydrocarbons was registered for obtained bio-oil samples, using 2NHZ as catalysts. The higher content of aldehydes, ketones, and hydrocarbons could be achieved by the direct contribution of Brønsted acid sites from zeolite samples, as reported elsewhere [40]. Furthermore, the lower composition of framework compensation cations on the 2NHZ zeolite sample might improve chemical species diffusion into the zeolite framework. Then, generated species from biomass pyrolysis can reach Brønsted acid sites without difficulty, resulting in new species after an adsorbate-site interaction. The contribution of a lower composition of compensation cations to a higher diffusion into Chilean natural zeolites pores was reported elsewhere [41]. However, a higher composition of phenols was observed in obtained bio-oil, using NHZ sample, which is probably due to the lower Brønsted acid site density of this sample and a channel blockade as a result of applied chemical treatment. As mentioned before, aldehydes react with phenols. Thus, a lower content of aldehydes and a higher content of phenols in obtained bio-oil using NHZ sample is a logical outcome.



Scheme 1. Simplified reaction pathways of catalytic biomass pyrolysis. Adapted from [40,42–44].

Table 4. Main components of bio-oil obtained from catalytic Oak pyrolysis at 723 K.

*Fam	Compounds	% Area			Compounds	% Area		
		NZ	NHZ	2NHZ		NZ	NHZ	2NHZ
Ald	Butanedial			0.21	2,5-Dimethoxy-4-methylbenzaldehyde	0.88	0.76	
	Syringaldehyde	0.26			2-Furancarboxaldehyde, 5-methyl-			0.23
	Furfural	0.56	0.40	31.03	4-Hydroxy-2-methylbenzaldehyde			0.42
	Furfural, 5-methyl-	0.41	2.17		2,5-Dimethoxy-4-ethylbenzaldehyde	3.62	0.88	
Ket	Acetosyringone	0.68			2-Cyclopenten-1-one, 3,4-dimethyl-			0.72
	1,2-Cyclopentanedione			0.66	2-Cyclopenten-1-one, 3,5,5-trimethyl-			4.81
	Guaiacylacetone	0.55	0.46		2H-Pyran-2-one, 3-acetyl-4-hydroxy-6-methyl-			7.52
	2-Cyclopentene-1,4-dione			0.55	Ethanone, 1-(4-hydroxy-3-methoxyphenyl)-	0.15	0.16	
	2(5H)-Furanone, 5-methyl-			0.27	3,4-Dihydro-6-methyl-2H-pyran-2-one			0.51
	2-Cyclohexen-1-one, 2-methyl-			0.23	3-Cyclopenten-1-one, 2,2,5,5-tetramethyl-			0.34
	1,3-Cyclopentanedione, 2-ethyl-			0.94	3H-Pyrazol-3-one, 2,4-dihydro-2,4-dimethyl-			0.28
	2-Cyclopenten-1-one, 2-hydroxy-		1.12		3H-Pyrazol-3-one, 2,4-dihydro-2,5-dimethyl-			1.75
	2-Acetyl-5-methylfuran			7.10	3-methyl-1, 2-cyclopentanedione	0.88	1.58	
	Est	1-Propionylethyl acetate			0.87	Propanoic acid, ethenyl ester	0.27	0.17
Butyric acid, neopentyl ester				0.17	Tricosanoic acid, methyl ester	33.33	0.18	
Eth	Benzene, ethoxy-			0.74	Benzene, 2-ethoxy-1,3-dimethoxy-			13.72
	1,2,4-Trimethoxybenzene	6.43	5.37		1,2,3-Trimethoxy-5-methylbenzene	13.94	11.06	
	Benzene, 1-ethoxy-4-methyl-			1.14	Ether, 3-butenyl propyl			0.17
HC	Hexacosane	0.17	0.22	0.56	Nonacosane		0.13	0.45
	4-Decene, 3-methyl-, (E)-			0.19	Octacosane	0.15		0.51
	Docosane	0.23	0.39	0.40	Pentacosane	0.29	0.64	0.72
	Heneicosane		0.23	0.12	Tetracosane	0.45	0.38	0.92
	Hentriacontane			0.33	Triacotane			0.39
	Heptacosane	0.25	0.38	0.52	Tricosane	0.33		0.69
	Phe	Phenol, 2-methoxy-	1.47	4.05	5.29	Phenol, 2-methoxy-3-(2-propenyl)-		0.57
2-Isopropoxyphenol				0.42	Phenol, 2-methoxy-4-methyl-		3.32	1.13
2-Methoxy-4-vinylphenol		0.80	1.04		Phenol, 2-methyl-		0.78	
2-Methoxy-5-methylphenol				0.51	Phenol, 3,4-dimethoxy-	0.36	1.09	
4-Ethylguaiaicol		0.38	6.43		Phenol, 3,4-dimethyl-		0.76	0.08
Desaspidinol		1.17	1.11		p-Methylguaiaicol	1.54	5.65	
Eugenol			0.54		p-Propylguaiaicol		0.85	
Homopyrocatechol		0.29	1.25		Pyrocatechol	0.42	2.22	
Isoeugenol		7.76	7.23		Pyrocatechol, 3-methoxy-	0.61	2.19	
Methoxyeugenol		1.40	0.91		Pyrocatechol, 3-methyl	0.13	1.14	
Phenol		0.14	0.38		Syringol	9.24	14.97	

*Fam: Families; Ald: Aldehydes; Ket: Ketones; Est: Esters; Eth: Ethers; HC: Hydrocarbons; Phe: Phenols.

Chemical species within the zeolite framework are subjected to interactions with Brønsted acid sites. As a result of those interactions, Cellulose is decomposed (by a depolymerisation process through transglycosylation) into aldehydes, anhydrosugars (mainly levoglucosan), ketones, and alcohols. Hemicellulose is transformed into pyrans and furans, and Lignin is converted into phenols [45]. Thus, the interaction of adsorbed chemical species with Brønsted acid sites of zeolite samples, lead to the generation of hydrocarbons, carbon monoxide, carbon dioxide, water, and coke formation through several ring-opening reactions [45]. Another route goes from anhydrosugars, obtained from the cellulose upon pyrolysis, to furans by a rearrangement. Then, furans initiate a sequence of reactions that lead to hydrocarbons as well. A general idea of the abovementioned potential reaction pathways is illustrated in Scheme 1.

Based on experimental results obtained here, Chilean natural and modified zeolites lead to intermediates, such as aldehydes, ketones, ethers, phenols, and aliphatics. Thus, Chilean zeolites could be considered as an alternative catalyst for the obtention of sustainable value-added chemical compounds. On the other hand, synthetic zeolites usually lead to an increase of aromatics compounds in the bio-oil composition, due to their crystalline structure [46,47]. Moreover, the mesoporous and acidic zeolites lead to the production of shorter chain hydrocarbon due to their high cracking ability. Furthermore, microporous and less acidic zeolites favor the production of long chain hydrocarbons as the cracking process occurred mainly on the zeolite external surface [48]. Finally, reported hydrocarbons

(HC) fractions in Table 4, using 2NHZ, confirmed the abovementioned affirmations since C15-C30 hydrocarbons were registered in acquired chromatographic data.

The GC/MS procedure identified a large number of chemical compounds, after interpretation of registered data, using the automatic library search from National Institute of Standards and Technology (NIST) 2008. As a consequence of natural and modified zeolite catalytic activity, the composition of obtained bio-oils varies from one sample to the other, as Table 4 shows. Chemicals summarised here, are mainly oxygenated species with different functional groups including hydroxyl, phenolic hydroxyl, carboxyl, carbonyl, methoxy, ethoxy, oxygen-containing heterocyclic and unsaturated double bonds. Similar compounds were reported elsewhere [49–51].

The highest composition of furfural in obtained bio-oil samples was obtained when 2NHZ zeolite sample was used. The furfural composition was increased by several times, compared with those obtained when the parent natural zeolite sample was used. As reported in Table 3, the 2NHZ zeolite sample poses a higher density of Brønsted, among all samples analyzed in this study. Consequently, the increase of furfural composition can be associated with the incorporation of Brønsted acid sites in the 2NHZ sample. Brønsted acid sites were linked to the improvement of the degradation of polysaccharides to intermediates for furfural. Then, modified natural zeolites can be considered as a potential catalyst to obtain furfural via catalytic pyrolysis of biomass. As a value-added chemical, furfural is a relevant by-product of bio-oil, and it is widely used in medicines, resins, food additives, and fuel additives manufacture [52].

As mentioned before, bio-oil quality can be improved through deoxygenation reactions using Brønsted acid sites of zeolites, to obtain lower oxygenated compounds in bio-oil. Thus, a qualitative analysis was conducted to confirm the catalytic activity of zeolite samples. Table 5 shows a qualitative compositional analysis of obtained bio-oil samples, using natural and modified zeolite samples on the Oak catalytic slow pyrolysis investigated in this study.

Table 5. Qualitative analysis of bio-oil obtained from catalytic Oak pyrolysis.

Compounds	Percentage [%]		
	NZ	NHZ	2NHZ
Oxygenated	66.0	63.8	46.8
Non-oxygenated	17.0	14.5	14.4
Unknown	17.0	21.7	38.7

As Table 5 shows, a lower percentage of oxygenated compounds was registered in the bio-oil samples from catalytic assays using the 2NHZ sample. The lower percentage of oxygenated compounds can be associated with surface reactions promoted by Brønsted active acid sites in the modified zeolite framework [9,53]. Thus, the surface Brønsted acid sites possess a significant role in the catalytic pyrolysis, leading the transformation of original species from Oak pyrolysis to valuable by-products (hydrocarbons, aldehydes, and ketones).

Oxygenated species have several unsaturated bonds, which are responsible for several reactions in stored bio-oils. Moreover, a lower content of oxygenated compounds is required to avoid aging issues during bio-oils storage, considering the primary reactions of bio-oil aging (esterification, transesterification, homopolymerization, hydration, hemiacetal formation, acetalization, and phenol/aldehyde reactions) [18].

3. Materials and Methods

Biomass samples from a Chilean native oak tree (donated by Miraflores Angol Ltda., Angol, Chile) were subjected to size reduction ($d_p < 2$ mm), oven-dried at 313 K for 48 h and stored in a desiccator until further use. Samples were characterized by standard methods to obtain: humidity (Una Norma Española-European Norm (UNE-EN) 14774), ash content (UNE-EN 14775), calorific value (UNE-EN 14918), elemental analysis (UNE-EN 15104) and proximate analysis (American Society of

Testing Materials (ASTM) D 3172-73(84)) [54,55]. Thermogravimetric analysis was conducted in a thermobalance (Shimadzu DTG-60H, CROMTEK, Santiago, Chile).

Chilean natural zeolite (14% clinoptilolite, 74% mordenite, 12% quartz) was obtained from Minera FORMAS, Santiago, Chile. Zeolite samples were ground and sieved to 0.3 to 0.425 mm, then rinsed with ultrapure water (from an EASY pure RF II system), oven-dried at 398 K for 24 h, and stored in dry conditions. First, ammonium-modified zeolites were obtained from natural zeolite by an ion-exchange procedure with ammonium sulfate ($0.1 \text{ mol}\cdot\text{dm}^{-3}$), using a solution/solid ratio of 10:1 in a temperature-controlled water bath at 363 K for 3 h. Finally, modified samples were rinsed with ultra-pure water for 4 h, replacing the water at 2 and 3 h. The sample obtained here was named as NHZ. A second ammonium-modified zeolite sample (2NHZ) was obtained from NHZ, applying the same aforementioned ion-exchange procedure. More details can be found in a previous article [18]. Lastly, zeolite samples were oven-dried at 378 K for 24 h and stored in a desiccator until further use.

To characterize zeolite samples, the following quantitative methods were conducted: nitrogen absorption at 77 K, XRD, and XRF. The surface area was calculated from adsorption isotherms data, obtained with a Micromeritics Gemini 3175 (UDEC, Concepción, Chile).

To evaluate mineralogical content and structural framework of zeolite samples, XRD analysis was performed using a Bruker AXS Model D4 ENDEAVOR diffractometer (UDEC, Concepción, Chile), equipped with a copper X-ray tube and a Ni filter. Powdered natural and modified zeolite samples were mounted on quartz plates and stepped scanned over the angular range of 3 to 70° (2θ), a step size of 0.02 and a time/step of 0.2 s. X-ray generator was fixed at 40 kV and 20 mA. In the same way, X-ray fluorescence allowed the determination of the bulk chemical composition of natural and modified zeolite samples, using a RIGAKU Model 3072 spectrometer (UDEC, Concepción, Chile). Characterization procedures were reported elsewhere [29,56,57].

A procedure was developed to confirm the nature and strength of zeolite acid sites using pyridine as a probe molecule. In contrast to NH_3 -TPD, pyridine adsorption discriminates between Lewis and Brønsted sites. The pyridine adsorption was followed by DRIFT using a Nicolet (Alta Tecnología, Chile) Avatar 370 MCT with a smart collector accessory, a mid/near-infrared source, and a mercury cadmium telluride (MCT-A) photon detector at 77 K (liquid N_2), according to the procedure reported before [18].

A quartz cylindrical reactor was used in the experimental pyrolysis system, as shown in Figure 3. Biomass samples (9 g) were heated (ramp rate $10 \text{ K}\cdot\text{min}^{-1}$) from room temperature to 623 K and kept isothermal for 30 min under a nitrogen flow rate of $60 \text{ cm}^3\cdot\text{min}^{-1}$. Zeolite samples were out-gassed at 623 K for 2 h before pyrolysis experiments. Bio-oils were obtained after condensation of pyrolysis vapors in a closed flask at 253 K. Pyrolysis product fractions (bio-oil and biochar) were quantified gravimetrically, and the gaseous fraction was calculated by difference.

As known, a large number of chemical species were commonly identified in bio-oil samples. Thus, a fractionation method was conducted here to separate some of the wood-extractive derived compounds in seven fractions, considering reported articles before [25,58,59]. Bio-oil samples were diluted (ratio 1:1) with ultrapure water and centrifuged at 3300 rpm for 5 min in an LW SCIENTIFIC (Santiago, Chile) ULTRA 8V apparatus. After removal of the water-soluble supernatant, the water-insoluble phase of the bio-oil samples was placed in an solid-phase extraction (SPE) cartridge (UCT-CUSIL 500 mg/10 cm^3). Then, the SPE column was eluted (using a manifold vacuum system) with 10 cm^3 of each solvent (Lichrosolv grade) according to the following sequence: hexane, cyclohexane, diethyl ether, dichloromethane, ethyl acetate, acetone, and acetonitrile. Eluted samples from SPE cartridge were investigated by GC/MS to identify chemical species, using a Shimadzu (Cromtek, Chile) QP2010-plus apparatus. GC/MS was configured following the procedure reported elsewhere [18]. Chromatographic data were processed using GCMSsolution (v2.53) (Shimadzu, Santiago, Chile) and mass spectra laboratory databases (NIST08 and NIST08s).

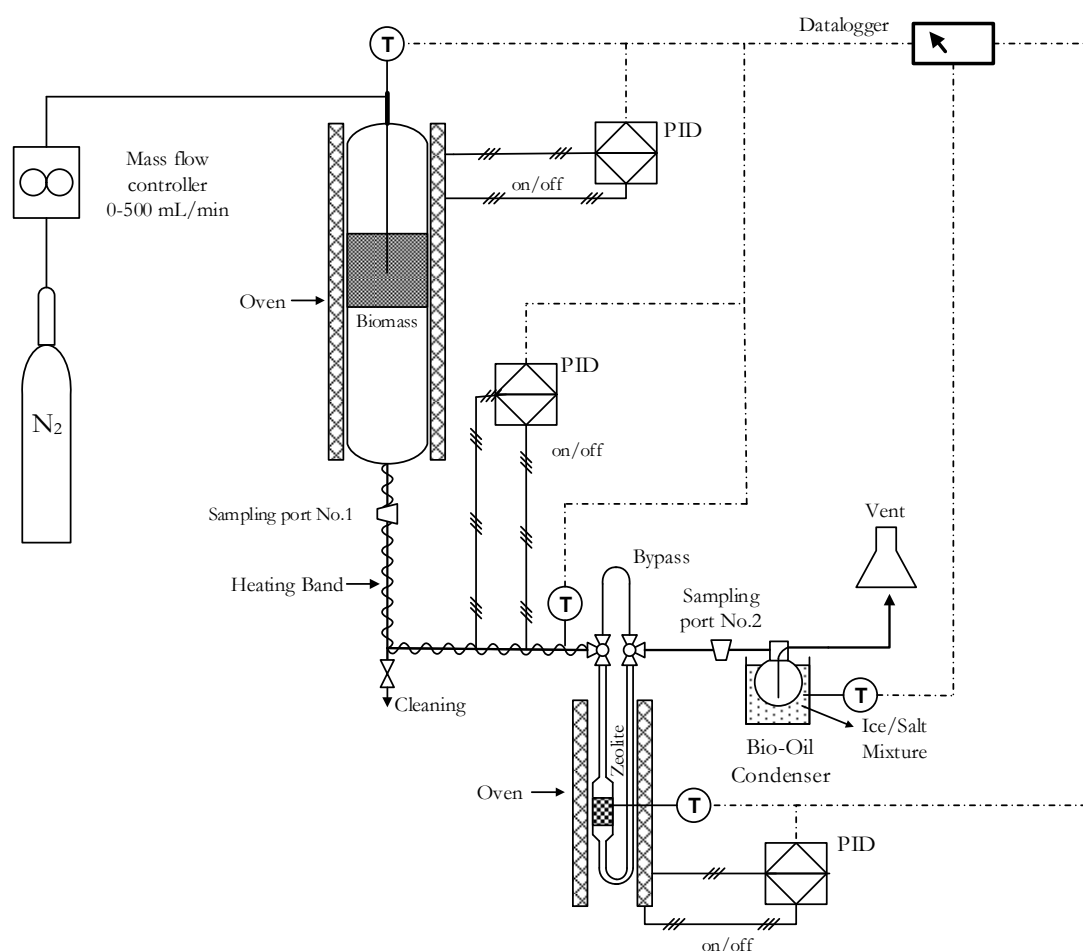


Figure 3. Experimental setup.

4. Conclusions

The catalytic pyrolysis of Chilean Oak over natural and modified zeolites was investigated in this study. As demonstrated here, the acidity of modified zeolites changed the reaction chemistry and products distribution. The Brønsted acid sites on ammonium-modified zeolite samples are responsible for the upgraded bio-oil and value-added chemicals, obtained in this research. Bio-oil chemical composition was modified when the pyrolysis-derived compounds were upgraded over 2NHZ zeolite sample, leading to a lower quantity of oxygenated compounds and a higher composition of value-added chemicals (e.g., furfural), among other compounds. Consequently, modified Chilean natural zeolites can be considered as a potential catalyst to obtain value-added chemicals via catalytic pyrolysis of biomass.

Author Contributions: S.A.-M., A.M.A., and H.D.P. conceived and designed the experiments, A.M.A. and H.D.P. performed the experiments, S.A.-M., A.M.A., and C.C.-B. analyzed the data, S.A.-M. and A.M.A. wrote the paper.

Funding: This research was funded by the Chilean National Fund for Scientific and Technological Development (Fondecyt Grant No. 11140781, Fondecup Grant No. 170077), the Nanomaterials and Catalysts for Sustainable Processes (NanoCatpPS) research group from University of Bio-Bio, Chile and the University of Bio-Bio, Concepción, Chile.

Acknowledgments: The authors wish to acknowledge to Daniel J. Nowakowski and Scott W. Banks from EBRI, Aston University in Birmingham U.K., for this valuable collaboration on the DRIFT experiments.

Conflicts of Interest: The authors declare no conflict of interest. The founding sponsors had no role in study design, collection, analyses, and interpretation of data, manuscript writing, the decision to publish the results.

References

1. Borsatto, F.; Inglezakis, V.J. Natural zeolite markets and strategic considerations. In *Handbook of Natural Zeolites*; Bentham Science Publishers: Bacau, Romania, 2012; pp. 11–27. ISBN 9781608054466.
2. Fankhauser, S.; Jotzo, F. Economic growth and development with low-carbon energy. *Wiley Interdiscip. Rev. Clim. Chang.* **2017**, *9*, e495. [CrossRef]
3. Zeng, S.; Liu, Y.; Liu, C.; Nan, X. A review of renewable energy investment in the BRICS countries: History, models, problems and solutions. *Renew. Sustain. Energy Rev.* **2017**, *74*, 860–872. [CrossRef]
4. Rahman, F.A.; Aziz, M.M.A.; Saidur, R.; Bakar, W.A.W.A.; Hainin, M.R.; Putrajaya, R.; Hassan, N.A. Pollution to solution: Capture and sequestration of carbon dioxide (CO₂) and its utilization as a renewable energy source for a sustainable future. *Renew. Sustain. Energy Rev.* **2017**, *71*, 112–126. [CrossRef]
5. Demirbaş, A.; Arin, G. An overview of biomass pyrolysis. *Energy Sources* **2002**, *24*, 471–482. [CrossRef]
6. Papari, S.; Hawboldt, K. A review on condensing system for biomass pyrolysis process. *Fuel Process. Technol.* **2018**, *180*, 1–13. [CrossRef]
7. Hosoya, T.; Kawamoto, H.; Saka, S. Solid/liquid- and vapor-phase interactions between cellulose- and lignin-derived pyrolysis products. *J. Anal. Appl. Pyrolysis* **2009**, *85*, 237–246. [CrossRef]
8. Zanuttini, M.S.; Lago, C.D.; Querini, C.A.; Peralta, M.A. Deoxygenation of m-cresol on Pt/ γ -Al₂O₃ catalysts. *Catal. Today* **2013**, *213*, 9–17. [CrossRef]
9. Gurevich Messina, L.I.; Bonelli, P.R.; Cukierman, A.L. In-situ catalytic pyrolysis of peanut shells using modified natural zeolite. *Fuel Process. Technol.* **2017**, *159*, 160–167. [CrossRef]
10. Rezaei, P.S.; Shafaghat, H.; Daud, W.M.A.W. Production of green aromatics and olefins by catalytic cracking of oxygenate compounds derived from biomass pyrolysis: A review. *Appl. Catal. A Gen.* **2014**, *469*, 490–511. [CrossRef]
11. Mohammed, I.Y.; Kazi, F.K.; Yusup, S.; Alaba, P.A.; Sani, Y.M.; Abakr, Y.A. Catalytic intermediate pyrolysis of Napier grass in a fixed bed reactor with ZSM-5, HZSM-5 and zinc-exchanged zeolite-a as the catalyst. *Energies* **2016**, *9*, 246. [CrossRef]
12. Imran, A.; Bramer, E.A.; Seshan, K.; Brem, G. Catalytic flash pyrolysis of biomass using different types of zeolite and online vapor fractionation. *Energies* **2016**, *9*, 187. [CrossRef]
13. ACS Material Advanced Chemicals Supplier. Available online: <https://www.acsmaterial.com/materials/molecular-sieves.html> (accessed on 23 October 2018).
14. Inglezakis, V.J.; Zorpas, A.A. Physical and Chemical Properties. In *Handbook of Natural Zeolites*; EBooks, B., Ed.; Bentham Science Publishers: Bacau, Romania, 2012; pp. 70–102. ISBN 9781608052615.
15. Serrano, D.P.; Melero, J.A.; Morales, G.; Iglesias, J.; Pizarro, P. Progress in the design of zeolite catalysts for biomass conversion into biofuels and bio-based chemicals. *Catal. Rev.* **2018**, *60*, 1–70. [CrossRef]
16. Pütün, E.; Uzun, B.B.; Pütün, A.E. Fixed-bed catalytic pyrolysis of cotton-seed cake: Effects of pyrolysis temperature, natural zeolite content and sweeping gas flow rate. *Bioresour. Technol.* **2006**, *97*, 701–710. [CrossRef] [PubMed]
17. Aho, A.; Kumar, N.; Eränen, K.; Salmi, T.; Hupa, M.; Murzin, D.Y. Catalytic pyrolysis of woody biomass in a fluidized bed reactor: Influence of the zeolite structure. *Fuel* **2008**, *87*, 2493–2501. [CrossRef]
18. Alejandro-Martín, S.; Cerda-Barrera, C.; Montecinos, A.; Martín, S.A.; Cerda-Barrera, C.; Montecinos, A. Catalytic Pyrolysis of Chilean Oak: Influence of Brønsted Acid Sites of Chilean Natural Zeolite. *Catalysts* **2017**, *7*, 356. [CrossRef]
19. Ateş, F.; Pütün, A.E.; Pütün, E. Fixed bed pyrolysis of *Euphorbia rigida* with different catalysts. *Energy Convers. Manag.* **2005**, *46*, 421–432. [CrossRef]
20. Rajić, N.; Logar, N.Z.; Rečnik, A.; El-Roz, M.; Thibault-Starzyk, F.; Sprenger, P.; Hannevold, L.; Andersen, A.; Stöcker, M. Hardwood lignin pyrolysis in the presence of nano-oxide particles embedded onto natural clinoptilolite. *Microporous Mesoporous Mater.* **2013**, *176*, 162–167. [CrossRef]
21. Milovanovic, J.; Stensrød, R.; Myhrvold, E.; Tschentscher, R.; Stöcker, M.; Lazarevic, S.; Rajic, N. Modification of natural clinoptilolite and ZSM-5 with different oxides and studying of the obtained products in lignin pyrolysis. *J. Serbian Chem. Soc.* **2015**, *80*, 717–729. [CrossRef]
22. Corma Canos, A.; Iborra, S.; Velty, A. Chemical routes for the transformation of biomass into chemicals. *Chem. Rev.* **2007**, *107*, 2411–2502. [CrossRef]

23. French, R.; Czernik, S. Catalytic pyrolysis of biomass for biofuels production. *Fuel Process. Technol.* **2010**, *91*, 25–32. [[CrossRef](#)]
24. de Wild, P.; Reith, H.; Heeres, E. Biomass pyrolysis for chemicals. *Biofuels* **2011**, *2*, 185–208. [[CrossRef](#)]
25. Mohan, D.; Pittman, C.U.; Steele, P.H. Pyrolysis of Wood/Biomass for Bio-oil: A Critical Review. *Energy Fuels* **2006**, *20*, 848–889. [[CrossRef](#)]
26. Gregg, S.J.; Sing, K.S.W. *Adsorption, Surface Area and Porosity*; Academic Press: London, UK, 1982; ISBN 12-300950-2.
27. Englert, A.H.; Rubio, J. Characterization and environmental application of a Chilean natural zeolite. *Int. J. Miner. Process.* **2005**, *75*, 21–29. [[CrossRef](#)]
28. Christidis, G.E.; Moraetis, D.; Keheyan, E.; Akhalbedashvili, L.; Kekelidze, N.; Gevorkyan, R.; Yeritsyan, H.; Sargsyan, H. Chemical and thermal modification of natural HEU-type zeolitic materials from Armenia, Georgia and Greece. *Appl. Clay Sci.* **2003**, *24*, 79–91. [[CrossRef](#)]
29. Valdés, H.; Alejandro, S.; Zaror, C.A. Natural zeolite reactivity towards ozone: The role of compensating cations. *J. Hazard. Mater.* **2012**, *227–228*, 34–40. [[CrossRef](#)]
30. Alejandro, S.; Valdés, H.; Manero, M.-H.H.; Zaror, C.A.A. BTX abatement using Chilean natural zeolite: The role of Bronsted acid sites. *Water Sci. Technol.* **2012**, *66*, 1759–1769. [[CrossRef](#)] [[PubMed](#)]
31. Leliveld, B.R.G.; Kerkhoffs, M.; Broersma, F.A.; van Dillen, J.A.J.; Geus, J.W.; Koningsberger, D.C. Acidic properties of synthetic saponites studied by pyridine IR and TPD-TG of n-propylamine. *J. Chem. Soc. Trans.* **1998**, *94*, 315–321. [[CrossRef](#)]
32. Konan, K.L.; Peyratout, C.; Smith, A.; Bonnet, J.-P.; Magnoux, P.; Ayrault, P. Surface modifications of illite in concentrated lime solutions investigated by pyridine adsorption. *J. Colloid Interface Sci.* **2012**, *382*, 17–21. [[CrossRef](#)]
33. Simon-Masseron, A.; Marques, J.P.; Lopes, J.M.; Ribeiro, F.R.; Gener, I.; Guisnet, M. Influence of the Si/Al ratio and crystal size on the acidity and activity of HBEA zeolites. *Appl. Catal. A Gen.* **2007**, *316*, 75–82. [[CrossRef](#)]
34. Osman, A.I.; Abu-Dahrieh, J.K.; Rooney, D.W.; Halawy, S.A.; Mohamed, M.A.; Abdelkader, A. Effect of precursor on the performance of alumina for the dehydration of methanol to dimethyl ether. *Appl. Catal. B Environ.* **2012**, *127*, 307–315. [[CrossRef](#)]
35. Ajaikumar, S.; Pandurangan, A. Efficient synthesis of quinoxaline derivatives over ZrO₂/MxOy (M = Al, Ga, In and La) mixed metal oxides supported on MCM-41 mesoporous molecular sieves. *Appl. Catal. A Gen.* **2009**, *357*, 184–192. [[CrossRef](#)]
36. Karthik, M.; Magesh, C.J.; Perumal, P.T.; Palanichamy, M.; Arabindoo, B.; Murugesan, V. Zeolite-catalyzed ecofriendly synthesis of vibrindole A and bis(indolyl)methanes. *Appl. Catal. A Gen.* **2005**, *286*, 137–141. [[CrossRef](#)]
37. Kostyniuk, A.; Key, D.; Mdeleleni, M. Effect of Fe-Mo promoters on HZSM-5 zeolite catalyst for 1-hexene aromatization. *J. Saudi Chem. Soc.* **2018**. [[CrossRef](#)]
38. Tamura, M.; Shimizu, K.; Satsuma, A. Comprehensive IR study on acid/base properties of metal oxides. *Appl. Catal. A Gen.* **2012**, *433–434*, 135–145. [[CrossRef](#)]
39. Adam, J.; Blazsó, M.; Mészáros, E.; Stocker, M.; Nilsen, M.H.; Bouzga, A.; Hustad, J.E.; Gronli, M.; Oye, G. Pyrolysis of biomass in the presence of Al-MCM-41 type catalysts. *Fuel* **2005**, *84*, 1494–1502. [[CrossRef](#)]
40. Rahman, M.M.; Liu, R.; Cai, J. Catalytic fast pyrolysis of biomass over zeolites for high quality bio-oil – A review. *Fuel Process. Technol.* **2018**, *180*, 32–46. [[CrossRef](#)]
41. Alejandro, S.; Valdés, H.; Manero, M.-H.M.H.; Zaror, C.A. Oxidative regeneration of toluene-saturated natural zeolite by gaseous ozone: The influence of zeolite chemical surface characteristics. *J. Hazard. Mater.* **2014**, *274*, 212–220. [[CrossRef](#)]
42. Wang, K.; Kim, K.H.; Brown, R.C. Catalytic pyrolysis of individual components of lignocellulosic biomass. *Green Chem.* **2014**, *16*. [[CrossRef](#)]
43. Liu, S.-N.; Cao, J.-P.; Zhao, X.-Y.; Wang, J.-X.; Ren, X.-Y.; Yuan, Z.-S.; Guo, Z.-X.; Shen, W.-Z.; Bai, J.; Wei, X.-Y. Effect of zeolite structure on light aromatics formation during upgrading of cellulose fast pyrolysis vapor. *J. Energy Inst.* **2018**. [[CrossRef](#)]
44. Zheng, A.; Zhao, Z.; Chang, S.; Huang, Z.; Wu, H.; Wang, X.; He, F.; Li, H. Effect of crystal size of ZSM-5 on the aromatic yield and selectivity from catalytic fast pyrolysis of biomass. *J. Mol. Catal. A Chem.* **2014**, *383–384*, 23–30. [[CrossRef](#)]

45. Veses, A.; Aznar, M.; Martínez, I.; Martínez, J.D.; López, J.M.; Navarro, M.V.; Callén, M.S.; Murillo, R.; García, T. Catalytic pyrolysis of wood biomass in an auger reactor using calcium-based catalysts. *Bioresour. Technol.* **2014**, *162*, 250–258. [[CrossRef](#)]
46. Che, Q.; Yang, M.; Wang, X.; Chen, X.; Chen, W.; Yang, Q.; Yang, H.; Chen, H. Aromatics production with metal oxides and ZSM-5 as catalysts in catalytic pyrolysis of wood sawdust. *Fuel Process. Technol.* **2019**, *188*, 146–152. [[CrossRef](#)]
47. Che, Q.; Yang, M.; Wang, X.; Yang, Q.; Rose Williams, L.; Yang, H.; Zou, J.; Zeng, K.; Zhu, Y.; Chen, Y.; Chen, H. Influence of physicochemical properties of metal modified ZSM-5 catalyst on benzene, toluene and xylene production from biomass catalytic pyrolysis. *Bioresour. Technol.* **2019**, *278*, 248–254. [[CrossRef](#)]
48. López, A.; de Marco, I.; Caballero, B.M.; Laresgoiti, M.F.; Adrados, A.; Torres, A. Pyrolysis of municipal plastic wastes II: Influence of raw material composition under catalytic conditions. *Waste Manag.* **2011**, *31*, 1973–1983. [[CrossRef](#)] [[PubMed](#)]
49. Chen, D.; Zhou, J.; Zhang, Q.; Zhu, X. Evaluation methods and research progresses in bio-oil storage stability. *Renew. Sustain. Energy Rev.* **2014**, *40*, 69–79. [[CrossRef](#)]
50. Holladay, J.E.; White, J.F.; Bozell, J.J.; Johnson, D. Top Value-Added Chemicals from Biomass Volume II - Results of Screening for Potential Candidates from Biorefinery Lignin. *Pacific Northwest Natl. Lab.* **2007**, *II*, 87. [[CrossRef](#)]
51. Imam, T.; Capareda, S. Characterization of bio-oil, syn-gas and bio-char from switchgrass pyrolysis at various temperatures. *J. Anal. Appl. Pyrolysis* **2012**, *93*, 170–177. [[CrossRef](#)]
52. Zhang, H.; Liu, X.; Lu, M.; Hu, X.; Lu, L.; Tian, X.; Ji, J. Role of Brønsted acid in selective production of furfural in biomass pyrolysis. *Bioresour. Technol.* **2014**, *169*, 800–803. [[CrossRef](#)]
53. Mihalcik, D.J.; Mullen, C.A.; Boateng, A.A. Screening acidic zeolites for catalytic fast pyrolysis of biomass and its components. *J. Anal. Appl. Pyrolysis* **2011**, *92*, 224–232. [[CrossRef](#)]
54. Erol, M.; Haykiri-Acma, H.; Küçükbayrak, S. Calorific value estimation of biomass from their proximate analyses data. *Renew. Energy* **2010**, *35*, 170–173. [[CrossRef](#)]
55. Parikh, J.; Channiwala, S.A.; Ghosal, G.K. A correlation for calculating HHV from proximate analysis of solid fuels. *Fuel* **2005**, *84*, 487–494. [[CrossRef](#)]
56. Alejandro, S.; Valdés, H.; Zaror, C.A. Natural Zeolite Reactivity Towards Ozone: The Role of Acid Surface Sites. *J. Adv. Oxid. Technol.* **2011**, *14*, 182–189. [[CrossRef](#)]
57. Valdés, H.; Farfán, V.J.; Manoli, J.A.; Zaror, C.A. Catalytic ozone aqueous decomposition promoted by natural zeolite and volcanic sand. *J. Hazard. Mater.* **2008**, *165*, 915–922. [[CrossRef](#)] [[PubMed](#)]
58. Garcia-Perez, M.; Chaala, A.; Pakdel, H.; Kretschmer, D.; Roy, C. Characterization of bio-oils in chemical families. *Biomass and Bioenergy* **2007**, *31*, 222–242. [[CrossRef](#)]
59. Kanaujia, P.K.; Sharma, Y.K.; Garg, M.O.; Tripathi, D.; Singh, R. Review of analytical strategies in the production and upgrading of bio-oils derived from lignocellulosic biomass. *J. Anal. Appl. Pyrolysis* **2014**, *105*, 55–74. [[CrossRef](#)]

